Energy Storage Materials 21 (2019) 439–445

Contents lists available at ScienceDirect

Energy Storage Materials

journal homepage: www.elsevier.com/locate/ensm

High temperature solid-state supercapacitor designed with ionogel electrolyte

Bouchra Asbani [a,b], Camille Douard [a,b], Thierry Brousse [a,b], Jean Le Bideau [a,b,*]

[a] Institut des Matériaux Jean Rouxel (IMN), CNRS UMR 6502, Université de Nantes, Nantes, France
[b] Réseau sur le Stockage Electrochimique de l'Energie, CNRS FR, 3459, Amiens, France

ARTICLE INFO

Keywords:
Solid-state supercapacitor
Ionogel
Electrolyte
High temperature
Electrochemical double layer capacitor
Energy storage

ABSTRACT

To date, the design of high temperature electrochemical double layer capacitors (EDLCs) remains a challenge more specifically related to the electrolyte. The electrochemical performance of EDLC can be tuned by the temperature, and a better performance can be achieved at higher temperature if all the components are well suited to this purpose. Subsequently, an all solid-state EDLC operated at high temperature using porous carbon electrodes and a solid-like electrolyte was fabricated. Such an approach opens the route towards safer and flexible devices. An ionogel was used as the solid electrolyte and concomitantly as separator in this all-solid EDLC. The synthetized ionogel exhibits a high ionic conductivity over a wide temperature range, from 4 mS cm^{-1} at 20 °C up to 26 mS cm^{-1} cm at 100 °C. The all solid state EDLC thus prepared was able to withstand operating temperature as high as 100 °C, under a 2.5 V cell voltage. Long term galvanostatic charge−discharge cycling over 25 000 cycles were achieved at 100 °C, thus demonstrating very good capacitance retention. The ionogel-based EDLCs therefore appear to be suitable for high temperature environments.

1. Introduction

Electrochemical double-layer capacitors (EDLCs) also called supercapacitors (SCs) promise to play an important role in meeting the demands of electronic devices and integrated systems [1]. The use of such supercapacitor potentially enables far-reaching advances in backup energy storage and high pulse power applications like portable consumer electronics, memory back-up systems, military devices, space equipment, hybrid vehicles, next-generation all-electric cars, and large industrial scale power and energy management. EDLCs store energy using accumulation of ions at the interface between a highly porous carbon-based electrode and an electrolyte [2]. The charge storage mechanism is mainly capacitive with no chemical modification of the electrode involved during the charge/discharge process. As a result, EDLC can sustain millions of cycles, providing fast charge/discharge rates and subsequently high power density, while keeping a reasonable energy density.

The electrode materials of EDLCs must have a high specific surface area, which is of utmost importance to achieve high energy densities. Highly porous carbons, such as activated carbons, are commonly used as supercapacitor electrodes due to their high specific surface area and fair electronic conductivity [3–7]. Additionally, activated carbons can be used with a wide variety of electrolytes, including acidic and basic aqueous electrolytes, organic electrolytes and ionic liquid (ILs) [3].

Indeed, the electrolyte is the other core component of EDLCs, and must meet the requirements of high ionic conductivity and wide electrochemical stability potential window [8]. EDLCs employing activated carbon high surface area electrodes and conventional electrolytes such as $N(Et)_4BF_4$ in acetonitrile or propylene carbonate, represent the state of the art technologies currently on the market [1–5]. However, the use of such electrolyte leads to a number of safety issues and environmental drawbacks.

ILs are room temperature molten salts, entirely composed of cations and anions, the nature of which influences the chemical/electrochemical and physical properties [9]. For instance, the nature of the cation and the anion determines the potential window as well as the melting point or the viscosity, which in turn affects the ionic conductivity. Moreover, ILs typically show very low vapor pressure and high thermal stability, which allows high operating temperature [10]. Nevertheless, leakage still remains an issue with respect to their use in EDLCs since they are in a liquid state at room temperature. Additionally, most of EDLCs designed with ILs as electrolyte have been operated not higher than 80 °C [10–13], although with impressive cycling ability up to 150 000 cycles at 60 °C with activated carbon electrodes coupled with 1-ethyl-3-methylimidazolium

* Corresponding author. Institut des Matériaux Jean Rouxel (IMN), CNRS UMR 6502, Université de Nantes, Nantes, France.
E-mail address: jean.lebideau@cnrs-imn.fr (J. Le Bideau).

https://doi.org/10.1016/j.ensm.2019.06.004
Received 3 February 2019; Received in revised form 3 June 2019; Accepted 3 June 2019
Available online 10 June 2019

bis(trifluoromethylsulfonyl)imide (EMImTFSI) electrolyte [13]. Only few reports using various carbon electrodes including carbide derived carbons, bucky papers, or activated carbons demonstrate the possibility to increase the temperature up to 100 °C [14–18] or above (up to 140 °C) [19,20], but only few hundreds of cycles are shown. Moreover, the mass loading of the electrodes if either very low or unknown which makes the comparison with standard EDLC difficult and which gives some doubts about extrapolated power and energy densities as suggested in the literature [21,22].

In comparison to liquid electrolytes, designing solid electrolytes confining ILs, namely ionogels [23–26], is of great interest. ILs host networks can be silica based, polymer based, or hybrid organic-inorganic based. This approach enables to obtain solid like electrolyte with high ionic liquid content simultaneously with obtaining the separator. It avoids also leakage thus limiting packaging constraints and increasing the safety (no flammability nor vapor tension), while keeping good mechanical and thermal properties. It is worth noting that the ionogel can be also easily shaped for the desired application in supercapacitors [27–32].

Extending the temperature range is of great importance since this could solve the problem of operating EDLCs in severe conditions required for specific applications such as oil drilling, space hardware, high temperature manufacturing processes, etc. Thus, EDLCs with high energy and power densities that can withstand harsh temperature environments are extremely desirable. Moreover, to the best of our knowledge there is no systematic work on high temperature EDLCs, since the studies are usually limited to safe temperature operating window which does not exceed 60 °C as already mentioned above [10–13]. Indeed, it seems that an increase of temperature above 100 °C severely limits the safe operating voltage window which shrinks down to 0.5 V at 200 °C for EDLC operated with butyltrimethylammonium bis-(trifluoromethylsulfonyl) imide [20,33]. To date, thermally stable ionogels have been used as electrolytes in EDLCs and other devices requiring high temperatures [27]. Nevertheless, the operating temperature of ionogel electrolytes has been most often limited below 60 °C [29] even if some devices using an ionogel have demonstrated impressive cycling stability after being submitted to a solder reflow process at 260 °C for few minutes [30]. To the best of our knowledge, only one paper examines the use of physical gels using ILs (mixture of EMIm TFSI and SiO_2 particles) in an EDLC based on multi-walled carbon nanotubes electrodes operated at 100 °C [32]. However, the related device is also built with very low mass loading and only operated over a 2 V cell voltage, with a limited cycling ability of 2000 cycles.

In the present paper, we depict the concept of all solid state EDLCs that can sustain temperature as high as 100 °C over a large number of charge/discharge cycles. It combines two activated carbon electrodes assembled with an ionogel. This ionogel is obtained from a sol made of EMImTFSI, tetramethoxysilane (TMOS), dimethyldimethoxysilane (DMDMS) [30]. It is a key point that DMDMS affords flexibility to the silica matrix and enables the fabrication of a crack-free ionogel directly onto the carbon electrodes. This ionogel exhibits high ionic conductivity and good mechanical properties, and is thus suitable to be implemented in high temperatures all-solid-state EDLCs. These ionogel based EDLCs can be operated up to 3 V, demonstrating a high cycling stability (25 000 cycles) at 100 °C as well as a high specific capacitance. Such ionogel based EDLCs are intended for use at a high temperature.

2. Experimental

2.1. Carbon electrodes fabrication

Carbon electrodes were prepared using YP-50 (Kuraray) activated carbon powder (75 wt%) as the active material, carbon black Super-P (15 wt%) as a conductive additive and PVDF-HFP polymer as a binder (10 wt%). The PVDF was in suspension in N-methyl-2-pyrrolidone at 10 wt%. The mixture was blended under magnetic stirring during several hours. The obtained black paste was then casted on aluminum current collectors. Carbon electrodes were then dried out in a vacuum oven during 18 h at 100 °C. The mass loading was 9 mg cm^{-2}, determined by weighting the aluminum current collector before and after carbon casting.

2.2. Ionogel synthesis and casting

Ionogels were obtained from a sol made of tetramethoxysilane (TMOS ≥ 99%, Fulka), dimethyl-dimethoxysilane (DMDMS), formic acid (FA, ≥ 98%, Sigma Aldrich) and the IL 1-ethyl-3-methylimidazolium bis(trifluoromethylsulfonyl)imide (EMImTFSI 99.9%, Solvionic). The sol was stirred at room temperature for 5 min. The [TMOS/DMDMS]/IL:FA molar ratio was [70/30]/50:1. This composition allowed getting crack free solid electrolyte. The mixture was then casted on the carbon electrode and was aged for 2 days at room temperature. Concomitantly, a 2 mm thick self-standing ionogel is prepared with the same experimental conditions, for ionic conductivity measurements. This thick ionogel is left for aging 5 days at ambient temperature.

The obtained ionogel film on the carbon electrode was homogeneous and transparent. Then, the electrode underwent further drying at 0.5 mbar and 25 °C for 18 h. Electrodes assembling was performed in a glove box ($H_2O < 0.1$ ppm, $O_2 < 0.1$ ppm) using Swagelok cells with two stainless steel electrodes, without the need of a standard paper or polymer separator, nor extra step since with 50% of IL in these ionogels the surface is wetted by a nanometric layer of IL., and since these ionogels are soft and compliable.

2.3. Characterization

For the DSC measurements (Q20 calorimeter, TA Instrument), the samples were dried at 60 °C under vacuum (0.5 mbar) for 18 h and sealed in hermetic aluminum pans. Samples were then quenched to −150 °C at 40 °C.min^{-1} and heated from −150 to 50 °C at 5 °C.min^{-1} once the thermal equilibrium has been reached. TGA measurements were conducted from room temperature to 600 °C at 0.5 °C.min^{-1} under pure oxygen gas, after 30 min of stabilization at 40 °C. SEM observations were performed on cross sections of electrodes using a FEG-SEM Merlin Zeiss microscope.

Porosimetry measurements were performed using adsorption and

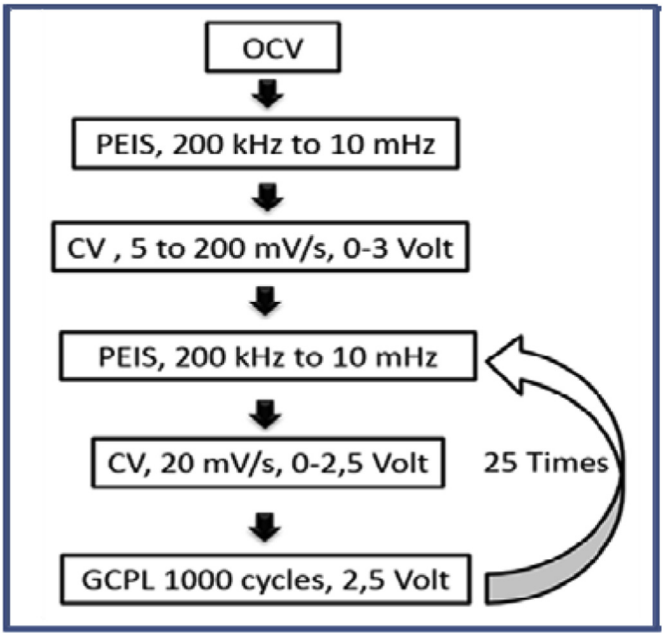

Fig. 1. Experimental process for the electrochimical characterizations of all solid state EDLCs.

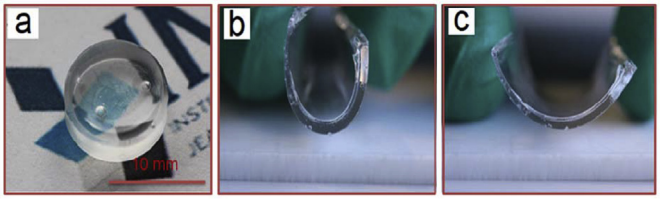

Fig. 2. (a) Bulk ionogel pellet and (b–c) film after aging, with molar ratio [70/30]/50.

desorption of gaseous nitrogen on the silica matrices obtained after IL extraction from the ionogel, by mean of Soxhlet apparatus with acetonitrile. The specific surface was obtained by the Brunauer-Emmett-Teller (BET) method. The pore size distribution and the pore volume were obtained by the Barett-Joyner-Halenda (BJH) method.

Potential Electrochemical Impedance Spectroscopy (PEIS) was used to determine the ionic conductivity in the temperature range −40 °C to +100 °C. Ionogel pellets were sandwiched between two stainless steel electrodes under argon atmosphere in a Swagelok-type cell. In case of IL alone, the measurement of the ionic conductivity requires the use of an additional Teflon ring. PEIS experiments were carried out in a frequency range from 200 kHz to 10 Hz with an amplitude of 50 mV and an acquisition rate of 6 points per decade. The ionic conductivity was calculated using the equation $\sigma = e/(RS)$, where e was the thickness (cm) of ionogel pellet, S was the geometric surface of ionogel and R (Ω) was the resistance, taken at the intersection of the Nyquist plot with the Z_{real} X-axis.

The electrochimical characterizations of solid state EDLCs were performed at 25 °C and at 100 °C according to sequence shown in Fig. 1, using a Swagelok cell with two stainless steel electrodes, using a VMP3 (Bio-Logic SA, France) potentiostat/galvanostat in order to evaluate the capacitance and the electrochemical stability window of the EDLCs. The electrochemical properties of EDLCs have been performed at 25 °C and 100 °C on the two symmetric electrodes (1.13 cm^2), both with the ionogel electrolytes facing each other and assembled in a Swaglock cell, without any additional separator. PEIS, Cyclic Voltammetry (CV) and Galvanostatic Cycling with Potential Limitation (GCPL) were evaluated on a Biologic VMP3 operated under EC-Lab software with a two electrodes configuration. PEIS experiments on EDLCs were carried out in a frequency range from 200 kHz to 10 mHz with an amplitude of 50 mV. Cyclic voltammograms were measured between 0 and 3 V using different scan rates of 5, 10, 20, 50, 100, 150 and 200 mV/s. Galvanostatic cycling GCPL has been performed on the EDLCs between 0 and 2.5 V with a constant charge discharge current ~1 A g^{-1}.

3. Results and discussion

Fig. 2(a–c) show ionogel pellet and film after 5 days aging at room temperature. A flexible material is obtained (Fig. 2 b-c). No leakage of liquid was observed even after several months.

The TGA thermograms of the IL and of the ionogel exhibit single step decomposition as depicted from Fig. 3a. For both, the mass are almost unchanged until 350 °C. Above 350 °C, monotonic decrease in weight loss is observed, similar to that of pure EMIm TFSI. As expected, the ionogel exhibits favorable thermal stability. The inception of thermal decomposition is detected at about 350 °C and complete degradation occurs at about 470 °C for EMIm TFSI and at 440 °C for the ionogel. In this last case the remaining weight corresponds to the silica scaffold which is not degraded upon heating the ionogel. Nevertheless the TGA results indicate that the ionogel possesses quite similar thermal stability than that of the corresponding IL, and thus it appears suitable for high temperature energy storage applications which is not possible for aqueous (<100 °C) or organic (<70 °C) based electrolytes [34,35], thus also avoiding leakage issue.

Fig. 3b displays the conductivity plot of the ionogel and of the non-confined IL, determined with PEIS. The ionic conductivity of pristine EMIm TFSI is 9 mS cm^{-1} at 20 °C, which is consistent with reported literature data [28,30]. For the ionogel with the composition [70/30]/50, the ionic conductivity is close to that of the corresponding IL between 20 °C and 100 °C. A value of 4 mS cm^{-1} was obtained at 20 °C. Noteworthy, this value increases up to 26 mS cm^{-1} at 100 °C. The ionic conductivity of the EMIm TFSI shows a break in the conductivity slope at −10 °C, corresponding to the phase transition from the liquid state to the solid state. The ionogel does not show such a break in the ionic conductivity which fades steadily as the temperature decreases down to

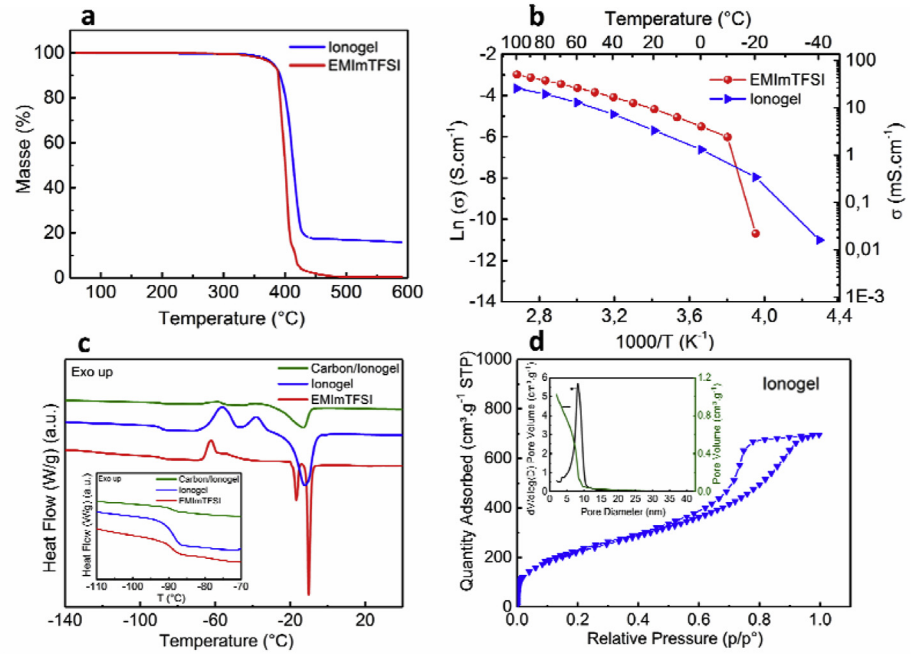

Fig. 3. (a) TGA showing thermal the thermal stability of the pristine IL and of the ionogel. (b) Conductivity versus temperature (c) DSC profiles of the IL and of the ionogel (d) N_2 adsorption/desorption isotherm; inset: BJH pore size distribution for the ionogel after IL extraction.

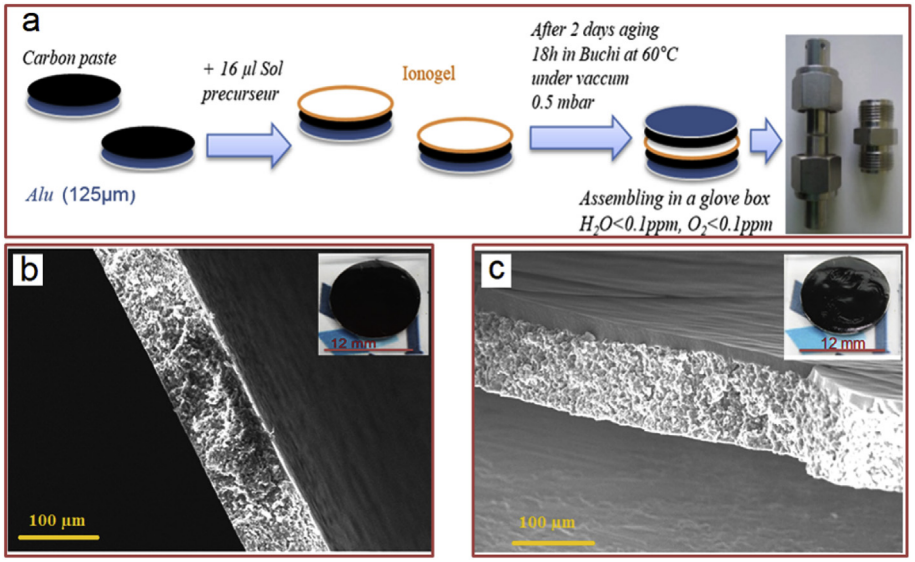

Fig. 4. (a) Schematic drawing of the fabrication process of an all-solid-state EDLC; SEM micrographs of the cross section of carbon electrode (b) before and (c) after ionogel casting, insets: carbon paste on 12 mm diameter aluminum current collector (125 µm thick) (b) before and (c) after ionogel casting.

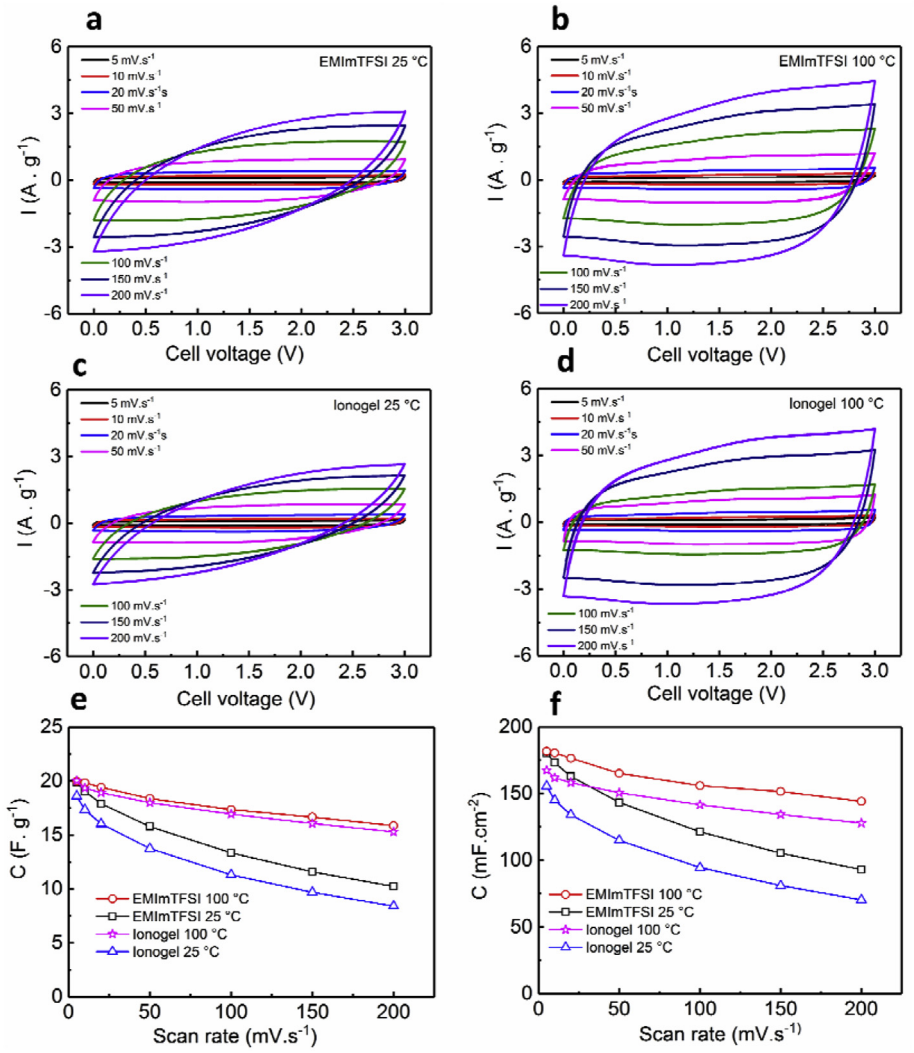

Fig. 5. Cyclic voltammetry data at different scan rates. (a) CVs at 25 °C and (b) CVs at 100 °C for the IL, (c) CVs at 25 °C and (d) CVs at 100 °C for the ionogel, (e) Gravimetric capacitance ($F.g^{-1}$) and (f) Areal capacitance ($mF.cm^{-2}$) *vs* scan rate at 25 °C and 100 °C for EDLCs with the IL and the ionogel.

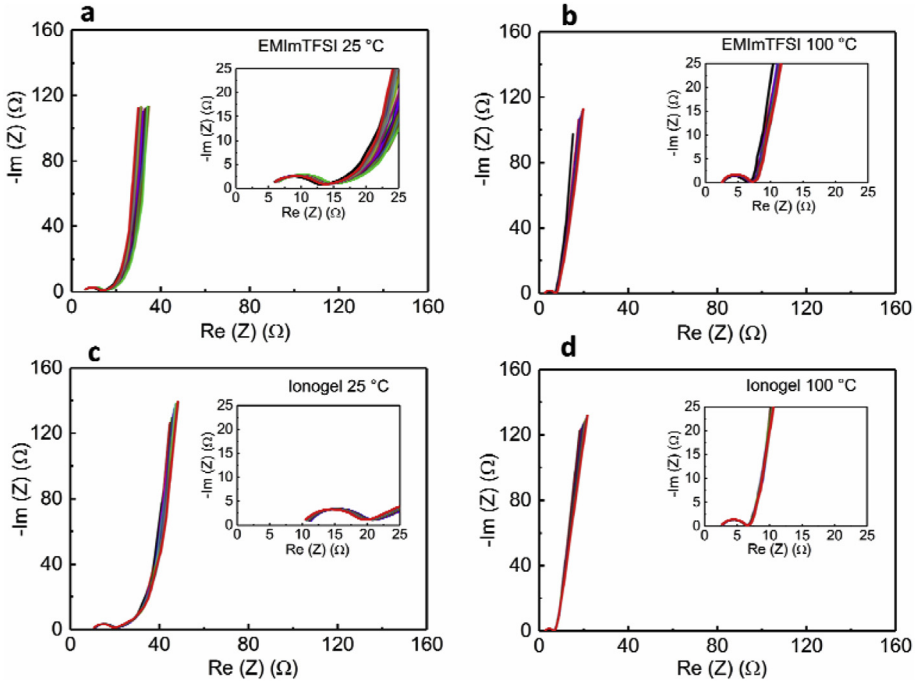

Fig. 6. Nyquist plot recorded after every 1000 GCPL cycles at room temperature (a, c) and 100 °C (b, d) for the IL (a, b) and for the ionogel (c, d) EDLCs.

−40 °C. This rather high ionic conductivity of the ionogel at low temperature is due to confinement effect, which quenches part, but not all, the liquid-to-solid transition [23]. The DSC measurements (inset in Fig. 3c) shows the glass transition temperature (T_g) of EMIm TFSI measured at −70 °C. The value of T_g decreases only slightly, likely within experimental error, with silica content, from −88 °C to −90 °C.

N_2-sorption measurements have been used to determine the surface area, pore volume and pore size distribution of the samples (Fig. 3d). The BET surface area is 800 ± 10 m^2 g^{-1}. From Fig. 3d it can be seen that the isotherm is of type IV with a typical hysteresis loop in a relative pressure range of 0.5–1.0, corresponding to a mesoporous structure [36]. Moreover, the inset in Fig. 3d shows the BJH pore size distribution plot with a maximum centered at ~8 nm.

The configuration of the all-solid-state EDLC is schematically shown in Fig. 4a. The ionogel acts as the electrolyte and also provides a physical barrier between electrodes to prevent short circuits. Fig. 4 b-c are the SEM cross sections of the carbon electrode before and after ionogel casting. The ionogel forms a 20 μm thick film on the surface of the carbon electrode.

Fig. 5a and b show CVs plots obtained with the IL and with the ionogel electrolyte at 25 °C and 100 °C over a 0–3 V voltage range at scan rates from 5 mV s^{-1} to 200 mV s^{-1}. At room temperature, the CVs (Fig. 5a) obtained with the IL exhibit a capacitive behavior as can be seen from the rectangular shapes of the CV. The CV shape of the all-solid-state EDLC with the ionogel is very similar (Fig. 5c). At 100 °C the CVs remain quasi-rectangular whatever the scan rate. Moreover, the improved ionic conductivity of the IL and of the ionogel at this temperature compared to that obtained at 25 °C provides a less distorted profile (Fig. 5b–d) thus indicating faster kinetic at high temperature, which was expected for such device. The gravimetric and areal capacitances at 25 °C and 100 °C for the all-solid-state EDLC are shown in Fig. 5e and f respectively. At low scan rates (5 mV s^{-1}), the gravimetric capacitance (20 F g^{-1}, total mass of both electrodes) and areal capacitance (177 mF cm^{-2}, total area of the device) measured at 25 °C for the EDLC based on the IL are in very good agreement with previously reported values using reasonable mass loadings (>2 mg cm^{-2}) [11–16]. It can be noted that the EDLCs based on the ionogel shows only a 10% difference at 25 °C with the EDLCs with the non-confined IL. Due to the low ionic conductivity of the electrolytes at room temperature, both devices (IL and ionogel based) exhibit a strong rate dependence of the capacitance which fades by 50% at 200 mV s^{-1}. When the cycling temperature is raised to 100 °C, the gravimetric and areal capacitances are very close for both devices and are increased by *ca* 5% compared to those at 25 °C. The capacitance decay upon increased cycling rate is also less drastic than at 25 °C, with almost 75% of the capacitance retained at 200 mV s^{-1} instead of 50% at 25 °C for the same cycling rate. Such behavior was not reported on previous study on ionogel-based EDLC [32] where capacitance still fade from 50% between 10 mV s^{-1} and 80 mV s^{-1}, when increasing the temperature from 25 °C to 100 °C. For this last case, this might be due to the physical gel (mixture of EMIm TFSI and SiO_2 particles) instead of the chemical gel (ionogel). With the ionogel, a better homogeneity is reached due to the impregnation of the sol on the carbon electrode, a better wetting of carbon particles is obtained, and a bicontinuous IL/host network interface is formed.

However, in our cell design, the thickness of the ionogel as a separator is 2 × 20 μm. At 100 °C, the resistance of such separator should be 0.14 Ω as determined from the ionic conductivity of the ionogel at 100 °C. However, from EIS analysis (Fig. 6), the resistance is 2.6 Ω. Thus it seems that the resistance of the cell is mainly due to ion diffusion in the porosity of the carbon of the electrodes. Moreover, when the temperature is raised from 25 °C up to 100 °C, the ionic conductivity of the ionogel increases by a factor of 6.5, but practically the cell resistance is only decreased by a factor of 4, thus pointing out again the role of ions diffusion in the carbon electrodes. The same remark applies for ionic liquid based cells. Indeed, Kuraray YP50 carbon is a microporous carbon with most of the pores below 2 nm and a cumulative pore volume close to 0.7 mL g^{-1} [37].

Fig. 6 shows Nyquist plots of carbon EDLCs with the IL and with the ionogel electrolytes at 25 °C and 100 °C, obtained before and after every CV and 1000 GCPL cycles. The proposed all solid state device is designed to be operated at high temperature; PEIS data below 25 °C are not shown here since they are of poor practical interest.

At medium frequencies region a small semi-circle is observed. The presence of a semi-circle has been reported by different authors using carbon based electrodes with IL or ionogel electrolyte [29,32]. Various explanations have been proposed including the carbon electrode/aluminum current collector interface [37,38] or the resistive-capacitive behavior of carbon electrodes at high frequencies for

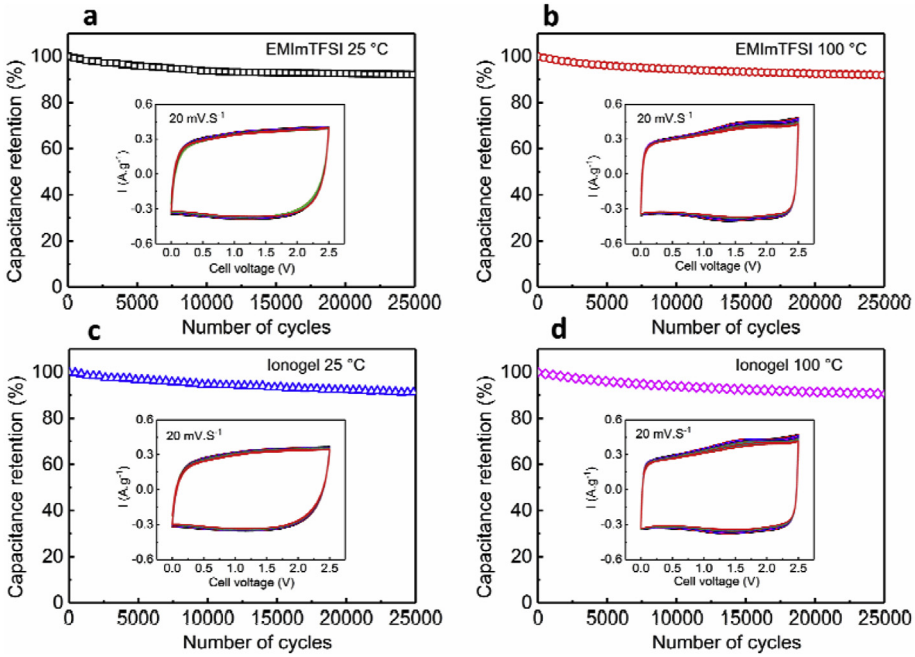

Fig. 7. GCPL data at room temperature (a, c) and 100 °C (b, d) for EDLCs using IL (a, b) and ionogel electrolytes (c, d); insets: CV at 20 mV s^{-1} recorded after every 1000 GCPL cycles according to the program presented Fig. 1; at the 25,000th cycle, the charge efficiency is of 78, 85, 73 and 83% for a, b, c, d *resp.*.

which the shape and width of these semicircles depend on the conductivity of the electrolyte at the electrode/separator interface and inside the separator [39]. Both explanations are provided by Soeda et al. and can be proposed in the case of our cells due to similarities with this last study [31].

For both EDLCs, all plots obtained at 25 °C and 100 °C show a diffusive behavior in the low frequency region. The slope of the 45° portion of the curve (Warburg impedance) is a result of the frequency dependence of ion diffusion/transport in the electrolyte confined in the porous carbon electrodes [2]. More interestingly is the decrease of the equivalent series resistance (ESR) from 5.5 to 2.5 Ω for the IL and from 10 to 2.6 Ω in for the ionogel based EDLC when the temperature increases from 25 °C to 100 °C. This clearly demonstrates that despite a higher ESR at 25 °C which will penalize the power density at room temperature compared to the device using IL impregnated in a standard separator, the ionogel electrolyte cancels this drawback at 100 °C with a similar ESR for both devices. Such interesting behavior for the solid state EDLC at 100 °C can be due to an improvement of the ionogel/electrodes interfaces, allowing fast ions transports from ionogel bulk electrolyte to the electrode surface at high temperature, as previously evidenced by our team [30].

Fig. 7 shows the cycling stability of the EDLCs at 25 °C and 100 °C for both IL and ionogel. The cell voltage was limited to 2.5 V in order to avoid the capacitance fade observed upon long term cycling tests using 3 V as upper cut-off voltage (not shown here). Such fade in capacitance when using a [0–3 V] cell voltage window can be due to the degradation of the electrolyte during cycling, or to the oxidation of the carbon electrode at the aluminum current collector at high temperature (100 °C), or coupled effects. As reported by some authors, at higher voltages, the deviations from ideal capacitive behavior are observed in CVs and PEIS data, and can be due to the specific adsorption of ions from the IL and/or to faradaic processes occurring on/inside carbon based electrodes based on the presence of undesirable traces of residual species (water, halogens) in the IL [39]. This observation is consistent with previously reported studies using ILs in EDLCs at high temperature, and concluding that the operating voltage window must be limited even to less than 1.2 V, in order to assume long term cycling when the operating temperature was raised up to 100 °C and above [32,33]. The insets of Fig. 7 present the CVs at 20 mV s^{-1} before and after every 1000 GCPL cycles. The solid state EDLC retains 92% of its initial capacitance after 25000 cycles, which reveals stable behavior for the electrode material and the ionogel electrolyte. These long term cycling abilities could be attributed to the limitation of the cell voltage at a maximum of 2.5 V, but it also evidences the good interface between the electrodes and the ionogel. It is the first time to our knowledge that such long term operation of EDLC using ILs and ionogels at 100 °C is reported in the literature. Former reports on ionogel-based EDLCs [32] have shown a capacitance retention of 88% after 2000 cycles.

4. Conclusion

A high-performance all-solid-state EDLC was designed with two activated carbon electrodes and an ionogel as the electrolyte. The all-solid-state supercapacitor has demonstrated very good performance at 25 °C and 100 °C compared to an EDLC using IL as electrolyte. The fabrication of such all-solid-state supercapacitor strongly depends on the ionogel with exhibit a wide electrochemical window (0–3 V) and a high ionic conductivity. Moreover, these performances are not degraded at 100 °C even with long term cycling tests thus demonstrating high thermal stability. In addition, the solid state EDLC exhibits very good long-term stability over 25 000 charge/discharge cycles which suggests a potential use in applications requiring mechanically stable devices that can be operated up to 100 °C. Further studies are in progress in order to evaluate the temperature stability of solid state EDLCs above 100 °C.

Data availability

The raw/processed data required to reproduce these findings cannot be shared at this time due to technical or time limitations.

Acknowledgment

The authors thank the French network on electrochemical energy storage (RS2E) for the financial support and gratefully acknowledge Kuraray Company for providing YP50 activated carbon. The authors also thank Fanch Guillou for providing special cell for testing EDLCs.

Appendix A. Supplementary data

Supplementary data to this article can be found online at https://doi.org/10.1016/j.ensm.2019.06.004.

References

[1] E. Frackowiak, F. Béguin, Supercapacitors: Materials, Systems and Applications, Wiley-VCH, Weinheim, Germany, 2013.
[2] B.E. Conway, Electrochemical Supercapacitors, Springer US, Boston, MA, 1999.
[3] E. Frackowiak, F. Béguin, Carbon materials for the electrochemical storage of energy in capacitors, Carbon 39 (2001) 937–950, https://doi.org/10.1016/S0008-6223(00)00183-4.
[4] E. Frackowiak, Carbon materials for supercapacitor application, Phys. Chem. Chem. Phys. 9 (2007) 1774–1785, https://doi.org/10.1039/B618139M.
[5] P. Simon, Y. Gogotsi, Materials for electrochemical capacitors, Nat. Mater. 7 (2008) 845–854, https://doi.org/10.1038/nmat2297.
[6] A. Davies, A. Yu, Material advancements in supercapacitors: from activated carbon to carbon nanotube and graphene, Can. J. Chem. Eng. 89 (2011) 1342–1357, https://doi.org/10.1002/cjce.20586.
[7] A. Borenstein, O. Hanna, R. Attias, S. Luski, T. Brousse, D. Aurbach, Carbon-based composite materials for supercapacitor electrodes: a review, J. Mater. Chem. A. 5 (2017) 12653–12672, https://doi.org/10.1039/C7TA00863E.
[8] C. Zhong, Y. Deng, W. Hu, J. Qiao, L. Zhang, J. Zhang, Review of electrolyte materials and compositions for electrochemical supercapacitors, Chem. Soc. Rev. 44 (2015) 7484, https://doi.org/10.1039/c5cs00303b.
[9] M. Armand, F. Endres, D.R. MacFarlane, H. Ohno, B. Scrosati, Ionic-liquid materials for the electrochemical challenges of the future, Nat. Mater. 8 (2009) 621–629, https://doi.org/10.1038/nmat2448.
[10] A. Brandt, S. Pohlmann, A. Varzi, A. Balducci, S. Passerini, Ionic liquids in supercapacitors, MRS Bull. 38 (2013) 554–559, https://doi.org/10.1557/mrs.2013.151.
[11] A. Balducci, R. Dugas, P.L. Taberna, P. Simon, D. Plée, M. Mastragostino, S. Passerini, High temperature carbon–carbon supercapacitor using ionic liquid as electrolyte, J. Power Sources 165 (2007) 922–927, https://doi.org/10.1016/j.jpowsour.2006.12.048.
[12] V. Ruiz, T. Huynh, S.R. Sivakkumar, A.G. Pandolfo, Ionic liquid–solvent mixtures as supercapacitor electrolytes for extreme temperature operation, RSC Adv. 2 (2012) 5591–5598, https://doi.org/10.1039/c2ra20177a.
[13] R. Thangavel, A.G. Kannan, R. Ponraj, V. Thangavel, D.-W. Kim, Y.-S. Lee, High-energy green supercapacitor driven by ionic liquid electrolytes as an ultra-high stable next-generation energy storage device, J. Power Sources 383 (2018) 102–109, https://doi.org/10.1016/j.jpowsour.2018.02.037.
[14] T. Sato, G. Masuda, K. Takagi, Electrochemical properties of novel ionic liquids for electric double layer capacitor applications, Electrochim. Acta 49 (2004) 3603–3611, https://doi.org/10.1016/j.electacta.2004.03.030.
[15] H. Kurig, A. Jänes, E. Lust, Electrochemical characteristics of carbide-derived carbon 1-Ethyl-3-methylimidazolium tetrafluoroborate supercapacitor cells, J.Electrochem. Soc. 157 3 (2010) A272–A279. https://doi.10.1149/1.3274208.
[16] C. Largeot, P.L. Taberna, Y. Gogotsi, P. Simon, Microporous carbon-based electrical double layer capacitor operating at high temperature in ionic liquid electrolyte, Electrochem. Solid State Lett. 14 (2011) A174–A176, https://doi.org/10.1149/2.013112esl.
[17] L. Dagousset, G. Pognon, G.T.M. Nguyen, F. Vidal, S. Jus, P.-H. Aubert, Electrochemical characterisations and ageing of ionic liquid/gbutyrolactone mixtures as electrolytes for supercapacitor applications over a wide temperature range, J. Power Sources 359 (2017) 242–249, https://doi.org/10.1016/j.jpowsour.2017.05.068.
[18] J.C. Varela, K. Sankar, A. Hino, X. Lin, W.-S. Chang, D. Coker, M. Grinstaff, Piperidinium ionic liquids as electrolyte solvents for sustained high temperature supercapacitor operation, Chem. Commun. 54 (2018) 5590, https://doi.org/10.1039/c8cc01093e.
[19] J. Jiang, High temperature monolithic biochar supercapacitor using ionic liquid electrolyte, J. Electrochem. Soc. 164 (2017) H5043–H5048, https://doi.org/10.1149/2.0211708jes.
[20] M. Haque, Q. Li, A.D. Smith, V. Kuzmenko, E. Köhler, P. Lundgren, P. Enoksson, Thermal influence on the electrochemical behavior of a supercapacitor containing an ionic liquid electrolyte, Electrochim. Acta 263 (2018) 249–260, https://doi.org/10.1016/j.electacta.2018.01.029.
[21] Y. Gogotsi, P. Simon, True performance metrics in electrochemical energy storage, Science 334 (2011) 917–918, https://doi.org/10.1126/science.1213003.
[22] A. Balducci, et al., A guideline for reporting performance metrics with electrochemical capacitors: from electrode materials to full devices, J. Electrochem. Soc. 164 (2017) A1487–A1488, https://doi.org/10.1149/2.0851707jes.
[23] A. Guyomard-Lack, P.-E. Delannoy, N. Dupré, C.V. Cerclier, B. Humbert, J. Le Bideau, Destructuring ionic liquids in ionogels: enhanced ionic liquid properties for solid devices, Phys. Chem. Chem. Phys. 16 (2014) 23639–23645, https://doi.org/10.1039/C4CP03187C.
[24] R. Göbel, R.J. White, M.-M. Titirici, A. Taubert, Carbon-based ionogels: tuning the properties of the ionic liquid via carbon–ionic liquid interaction, Phys. Chem. Chem. Phys. 14 (2012) 5992–5997, https://doi.org/10.1039/C2CP23929A.
[25] K. Zehbe, M. Kollosche, S. Lardong, A. Kelling, U. Schilde, A. Taubert, Ionogels based on poly(methyl methacrylate) and metal-containing ionic liquids: correlation between structure and mechanical and electrical properties, Int. J. Mol. Sci. 17 (2016) 391, https://doi.org/10.3390/ijms17030391.
[26] A. Guyomard-Lack, J. Abusleme, P. Soudan, B. Lestriez, D. Guyomard, J. Le Bideau, Hybrid silica–polymer ionogel solid electrolyte with tunable properties, Adv. Energy Mater. 4 (2014) n/a-n/a. doi 10.1002/aenm.201301570.
[27] S. Wang, B. Hsia, C. Carraro, R. Maboudian, High-performance all solid-state micro-supercapacitor based on patterned photoresist-derived porous carbon electrodes and an ionogel electrolyte, J. Mater. Chem. A. 2 (2014) 7997–8002, https://doi.org/10.1039/C4TA00570H.
[28] M. Brachet, T. Brousse, J. Le Bideau, All solid-state symmetrical activated carbon electrochemical double layer capacitors designed with ionogel electrolyte, ECS Electrochem. Lett. 3 (2014) A112–A115, https://doi.org/10.1149/2.0051411eel.
[29] L. Negre, B. Daffos, V. Turq, P.-L. Taberna, P. Simon, Ionogel-based solid-state supercapacitor operating over a wide range of temperature, Electrochim. Acta 206 (2016) 490–495, https://doi.org/10.1016/j.electacta.2016.02.013.
[30] M. Brachet, D. Gaboriau, P. Gentile, S. Fantini, G. Bidan, S. Sadki, T. Brousse, J. Le Bideau, Solder-reflow resistant solid-state micro-supercapacitors based on ionogels, J. Mater. Chem. A. 4 (2016) 11835–11843, https://doi.org/10.1039/C6TA03142K.
[31] K. Soeda, M. Yamagata, M. Ishikawa, Outstanding features of alginate-based gel electrolyte with ionic liquid for electric double layer capacitors, J. Power Sources 280 (2015) 565–572, https://doi.org/10.1016/j.jpowsour.2015.01.144.
[32] F.R. Ortega, J.P.C. Trigueiro, G.G. Silva, R.L. Lavall, Improving supercapacitor capacitance by using a novel gel nanocomposite polymer electrolyte based on nanostructured SiO2, PVDF and imidazolium ionic liquid, Electrochim. Acta 188 (2016) 809–817, https://doi.org/10.1016/j.electacta.2015.12.056.
[33] S. Fletcher, I. Kirkpatrick, R. Thring, R. Dring, J.L. Tate, H.R.M. Geary, V.J. Black, Ternary mixtures of sulfolanes and ionic liquids for use in high-temperature supercapacitors, ACS Sustain. Chem. Eng. 6 (2018) 2612–2620, https://doi.org/10.1021/acssuschemeng.7b04117.
[34] R.-S. Kühnel, N. Böckenfeld, S. Passerini, M. Winter, A. Balducci, Mixtures of ionic liquid and organic carbonate as electrolyte with improved safety and performance for rechargeable lithium batteries, Electrochim. Acta 56 (2011) 4092–4099, https://doi.org/10.1016/j.electacta.2011.01.116.
[35] A.B. McEwen, S.F. McDevitt, V.R. Koch, Nonaqueous electrolytes for electrochemical capacitors: imidazolium cations and inorganic fluorides with organic carbonates, J. Electrochem. Soc. 144 (1997) L84–L86, https://doi.org/10.1149/1.1837561.
[36] K.S.W. Sing, Reporting physisorption data for gas/solid systems with special reference to the determination of surface area and porosity (recommendations 1984), Pure Appl. Chem., PAC 57 (1985) 603–619, https://doi.org/10.1351/pac198557040603.
[37] S. Porada, D. Weingarth, H.V.M. Hamelers, M. Bryjak, V. Presser, P.M. Biesheuvel, Carbon flow electrodes for continuous operation of capacitive deionization and capacitive mixing energy generation, J. Mater. Chem. A. 24 (2014) 9313–9321, https://doi.org/10.1039/C4TA01783H.
[38] C. Portet, P.L. Taberna, P. Simon, C. Laberty-Robert, Modification of Al current collector surface by sol–gel deposit for carbon-carbon supercapacitor applications, Electrochim. Acta 49 (2004) 905–912, https://doi.org/10.1016/j.electacta.2003.09.043.
[39] H. Kurig, M. Vestli, A. Jänes E. Lust, Electrical double layer capacitors based on two 1-ethyl-3-methylimidazolium ionic liquids with different anions, Electrochem. Solid State Lett. 14 (2011) A120–A122, https://doi.org/10.1149/1.3596722.